

# Microfabricated Atomic Magnetometers

P. D. D. Schwindt, S. Knappe,\* V. Shah,\*

L. Hollberg, and J. Kitching

Time and Frequency Division, NIST

Boulder, CO 80305

[schwindt@boulder.nist.gov](mailto:schwindt@boulder.nist.gov)

\*Also with: University of Colorado, Boulder, CO 80309

L.-A. Liew and J. Moreland

Electromagnetics Division

NIST

Boulder, CO 80305

**Abstract**— Using the techniques of microelectromechanical systems, we are developing chip-scale atomic sensors based on laser excitation of alkali atoms. Recently, we demonstrated a magnetometer physics package based on coherent population trapping that had a sensitivity of 50 pT / Hz<sup>1/2</sup> at 10 Hz, had a volume of 12 mm<sup>3</sup>, and used 195 mW of power [1]. To improve the sensitivity and reduce the power consumption of the magnetometer, we are evaluating other methods of interrogating the atoms for use in microfabricated devices. One of these methods uses frequency modulated nonlinear magneto-optical rotation (FM NMOR). We demonstrate that an FM NMOR magnetometer can be made to self-oscillate, offering simple construction and low power consumption.

## I. INTRODUCTION

Applications ranging from mineral and oil exploration [2] and remote sensing to magnetocardiography [3] require measurements of the magnetic field with picotesla sensitivity or below. Optically pumped atomic magnetometers have long been an excellent choice for these applications due to their high accuracy, total field sensitivity, and relatively low power consumption [4]. However, many applications would benefit greatly if the size, power consumption, and cost of these magnetometers could be reduced. By taking advantage of the revolutionary techniques of microelectromechanical systems (MEMS), we are working to drastically miniaturize vapor-cell based atomic devices. We have constructed physics packages for both chip-scale atomic magnetometers (CSAMs) [1] and chip-scale atomic clocks (CSACs) [5] demonstrating reductions by orders of magnitude in size, weight, and power consumption while sacrificing little in performance when compared to currently available devices.

Most alkali atomic magnetometers work by measuring the precession (or Larmor) frequency of the spin of the unpaired electron in an alkali atom due to the presence of a magnetic field and therefore measure the magnitude of the magnetic field. The sensitivity of the magnetometer is determined by the signal-to-noise ratio with which the Larmor frequency is measured and the gyromagnetic ratio  $\gamma$  of the atom ( $\gamma = 7 \text{ Hz/nT}$  for <sup>87</sup>Rb). Our first CSAM measured the Larmor frequency indirectly by first measuring

the frequency difference between two magnetically sensitive hyperfine states and then subtracting the hyperfine frequency (6.8 GHz for <sup>87</sup>Rb) to obtain the Larmor frequency [6]. Although this CSAM performs reasonably well, measuring the Larmor frequency directly would offer improved sensitivity and eliminates the need for an oscillator operating at gigahertz frequencies. In future CSAMs we plan to implement a scheme that allows direct measurement of the Larmor frequency, and one technique that shows promise for use in a CSAM is frequency modulated nonlinear magneto-optical rotation (FM NMOR) [7]. We have implemented a table-top experiment to evaluate the technique of FM NMOR for use in miniature magnetometers, and we have shown that an FM NMOR magnetometer can be made to self-oscillate, eliminating the need for a local oscillator completely simplifying the control system for the magnetometer [8].

## II. THE CSAM PHYSICS PACKAGE

The magnetic sensor physics package that we have developed is shown in Fig. 1 and is constructed as follows: A vertical-cavity surface emitting laser (VCSEL) is mounted on a base plate patterned with gold conductors to carry electrical signals to and from the CSAM. A VCSEL is used because of its low power requirements (typically < 5 mW for most devices) and high modulation efficiency. Above the VCSEL a micro-optics package is mounted that attenuates the light power to 5  $\mu\text{W}$ , changes the beam polarization from circular to linear, and collimates the beam to a diameter of 170  $\mu\text{m}$ . Next a microfabricated rubidium vapor cell is mounted with a transparent indium-tin-oxide (ITO) heater placed above and below it. The ITO heaters dissipate 160 mW into the cell, heating it to 120 °C to create enough atomic density in the cell to absorb a significant fraction of the light. Finally, a *p-i-n* silicon photodiode is mounted above the cell to monitor the light transmission through the atomic vapor. All of the components of the CSAM are glued together with an optical epoxy, and gold wire bonds provide electrical connections to the base plate.

A key innovation enabling the CSAM was the development of MEMS based fabrication of the atomic vapor cells [9]. As opposed to traditional glass blown vapor cells, MEMS techniques allow the cells to be miniaturized to submillimeter sizes, lowering the power requirement for

---

This work was supported by the Microsystems Technology Office of the US Defense Advanced Research Projects Agency (DARPA).

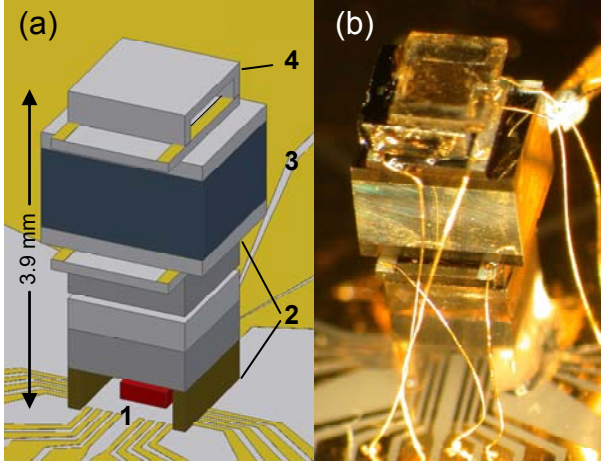


Figure 1. (a) Schematic and (b) photograph of the CSAM physics package. The components are: 1-VCSEL, 2-micro-optics, 3- $^{87}\text{Rb}$  vapor cell, 4-photodiode.

heating and allowing wafer-based production for easy integration with other components and the possibility of fabrication of multiple cells on a single wafer. The batch fabrication of cells and other components in wafers that are subsequently bonded together and then diced into individual CSAM devices would give substantial cost savings over individually assembled atomic magnetometers.

The Rb vapor cell is made by anodically bonding a glass wafer to either side of a 1 mm thick silicon wafer with a 1 mm<sup>2</sup> hole etched through it. The hole is made either with wet-chemical (KOH) or deep-reactive-ion etching. Before the second glass wafer seals the cell, the cavity in the Si wafer is filled with  $^{87}\text{Rb}$  and a buffer gas containing a mixture of argon at 11 kPa and neon at 21 kPa that reduces the frequency collisions between the Rb and the cell walls, which create decoherence of the spin precession.

As mentioned above the CSAM shown in Fig. 1 determines the magnetic field by measuring the hyperfine energy splitting between two magnetically sensitive states (Fig. 2(b)). We measure this microwave frequency using the

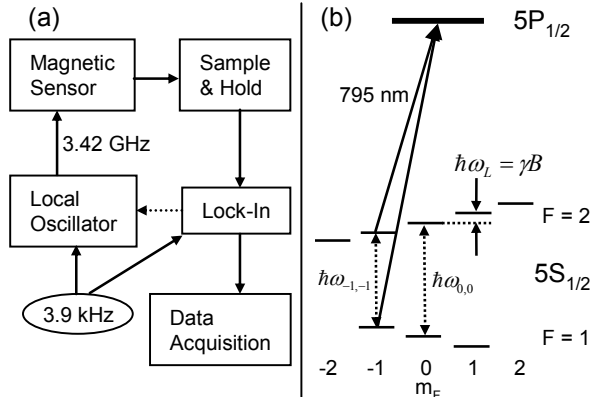


Figure 2. (a) The experimental setup for detecting the magnetic flux density. (b) Energy level diagram of  $^{87}\text{Rb}$  showing the resonant first-order sidebands of the VCSEL. The  $m_F = 0$  states are first-order insensitive to magnetic fields, whereas the  $m_F \neq 0$  states are.

all-optical method of coherent population trapping (CPT). To excite the CPT resonance, we tune the VCSEL to the D1 line of  $^{87}\text{Rb}$  at 795 nm. A local oscillator modulates the current to the VCSEL at 3.42 GHz, half the hyperfine splitting of the Rb ground state, creating two first-order sidebands that are simultaneously resonant between each hyperfine ground states and the  $P_{1/2}$  excited state (Fig. 2(b)). When the frequency difference between the first-order sidebands is equal to the splitting between two hyperfine states, the atoms are optically pumped into a coherent dark state. We then observe a reduction of the absorbed light power, for example, by 5.4 % when the current modulation frequency is tuned to the resonance, and the resonance width is 13 kHz. As shown in Fig. 2(b) two adjacent hyperfine resonances need to be measured to determine the Larmor precession frequency and thus the magnetic field.

To determine the center frequency of a particular CPT resonance, we employ phase sensitive detection by frequency modulating the local oscillator and sending the photodiode signal to a lock-in amplifier (Fig. 2(a)). The output noise spectrum of the lock-in is shown in Fig. 3 demonstrating a 50 pT Hz<sup>-1/2</sup> magnetic field sensitivity at 10 Hz bandwidth. The spikes in the noise spectrum at 20 Hz and above result from chopping the current to the ITO heaters on and off at 40 Hz. This is required because the magnetic field created by the heater currents is much larger than the ambient field and must be switched off while measuring the ambient field. The sample-and-hold circuit passes the photodiode signal to the lock-in only when the currents are off.

### III. CSAM IMPROVEMENTS

The present CSAM demonstrates a high sensitivity in a small 12 mm<sup>3</sup> package while dissipating 195 mW of power to operate the laser and heat the cell. Both the sensitivity and the power consumption are readily improved. Most of the power is used to heat the vapor cell, and with improved thermal design of the physics package, the power required for heating could be less than 10 mW, as demonstrated for a CSAC in [10]. The total power budget for a complete sensor must include the local oscillator and the control electronics. A local oscillator based on a micro-coaxial resonator operating at 3.4 GHz has been demonstrated to dissipate less

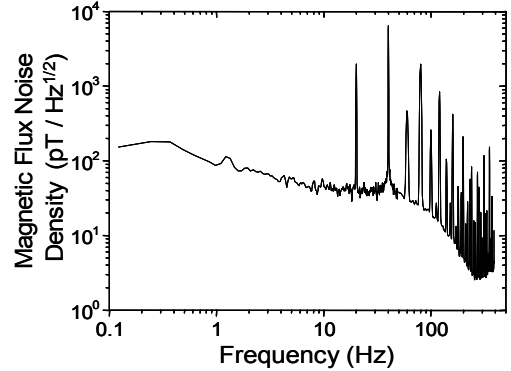


Figure 3. Power spectral density of the lock-in signal converted to units of magnetic flux density. The DC magnetic field is 73.9  $\mu\text{T}$ .

that 5 mW in a 0.1 cm<sup>3</sup> volume [11], and an application-specific integrated chip would provide low-power, small-size control of the CSAM. We envision an entire magnetometer that would occupy 1 cm<sup>3</sup> and dissipate less than 50 mW.

To improve the sensitivity of the magnetometer, it will be advantageous to implement a sensing scheme where the Larmor frequency is measured directly. The spin precession decoherence time is typically longer than the hyperfine decoherence time, giving narrower resonance lines and improving the sensitivity. Frequency stability of the small low-power local oscillator mentioned above currently limits the sensitivity of the CSAM. However, small oscillators that operate at the lower Larmor frequency provide sufficient stability, consume less power, and are readily available. Additionally, measuring the Larmor frequency directly eliminates the need to subtract two hyperfine frequencies. We expect that the sensitivity of a CSAM will approach 1 pT Hz<sup>-1/2</sup> using a direct Larmor measurement technique. Improvements in both sensitivity and bandwidth will also come from nonmagnetic heating of the CSAM.

#### IV. SELF-OSCILLATING FM NMOR MAGNETOMETER

Frequency modulated nonlinear magneto-optical rotation is a magnetometry technique proposed by Budker *et al.* [7] that we believe to be amenable to miniaturization. In FM NMOR linearly polarized light propagates along the direction of the magnetic field (Fig. 4), and the optical frequency of this light is modulated at twice the Larmor frequency moving it on and off the optical resonance of <sup>87</sup>Rb (D1 line,  $F = 2$  to  $F' = 1$ ). In highly miniaturized systems, the frequency modulation of the light can be accomplished through a modulation of the injection current of the laser. Frequency modulation eliminates the need for the traditional RF coil to excite the magnetic resonance, keeping the device as simple as possible. The linearly polarized light aligns the

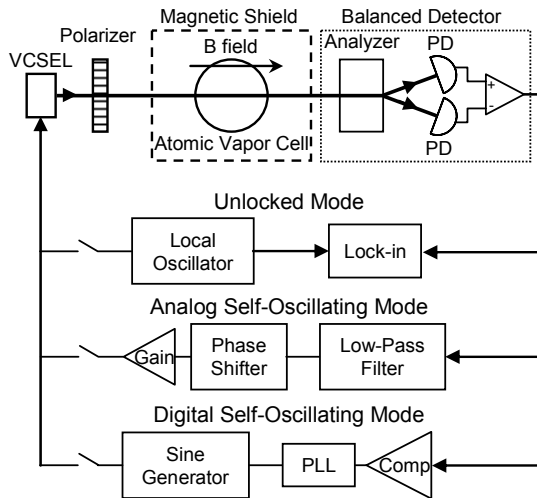


Figure 4. Schematic of the magnetometer. The difference signal from the two photo detectors (PDs) is sent to the various electronics required for operation in the different modes. The vapor cell is filled with isotopically enriched <sup>87</sup>Rb, coated with an anti-relaxation layer of paraffin, and has a diameter of 3.5 cm.

atomic spin along the direction of the light polarization, and as the atomic alignment precesses in the magnetic field, the frequency modulated light resonantly drives the alignment. The precessing atomic alignment in turn acts back on the light field rotating the light polarization, and this time-dependent rotation is read out by a balanced detector (Fig. 5). The use of a balanced detector offers the additional advantage of canceling much of the noise from the VCSEL. As was recognized long ago [4], further simplification of the magnetometer can be achieved if it can be made to self-oscillate, eliminating the need for a local oscillator. We have shown that the FM NMOR magnetometer can be made to self-oscillate in a table-top system, extending the usefulness of FM NMOR in a CSAM application by simplifying the control system and reducing the power consumption [8].

We operate the experiment in three modes: the unlocked mode, the analog self-oscillating mode, and digital self-oscillating mode (Fig. 4). In the unlocked mode, a local oscillator modulates the VCSEL current, and the FM NMOR signal is sent to a lock-in amplifier with the original modulation as the reference. When the frequency of the oscillator is swept about the FM NMOR resonance frequency, a dispersive line shape is observed at the in-phase output of the lock-in amplifier. The measured sensitivity of the magnetometer in the unlocked mode is plotted in Fig. 6 and is  $\sim 0.15$  pT Hz<sup>-1/2</sup> at 1 Hz bandwidth in a 143 nT field. A magnetometer using lock-in detection that automatically acquires and locks to the FM NMOR resonance would require the additional complication of a microprocessor.

To make the FM NMOR system self-oscillate, the output waveform from the balanced detector needs to emulate the input waveform before it is fed back to the VCSEL. As shown in the Fig. 5, the output waveform is not a simple replication of the input modulation, and in the analog self-oscillating mode we use a four-pole low-pass filter to attenuate all harmonics but the fundamental frequency. The roll-off frequency is set to 1.25 times the resonant frequency of the system (twice the Larmor frequency). With the phase

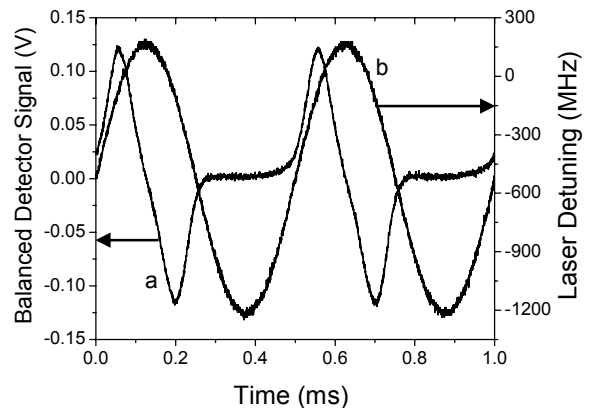


Figure 5. The FM NMOR signal (a) derived from the balanced detector is plotted as a function of time (unlocked mode), giving a measure of the optical rotation. The driving oscillator, modulating the laser frequency, is operating at 2 kHz, and the laser frequency relative to the peak of the optical transition is plotted (trace b).

## V. CONCLUSION

The CSAM is a promising sensor technology already showing good sensitivity from a small low-power physics package. The fabrication of the CSAM is compatible with wafer-level, mass fabrication techniques potentially reducing manufacturing costs. With good thermal packaging the power consumption of the sensor can be considerably reduced, and we expect to improve the sensitivity to  $1 \text{ pT Hz}^{-1/2}$  though a direct measurement of the Larmor frequency. An FM NMOR magnetometer in the self-oscillating configuration offers several advantages for use in a CSAM, including elimination of the local oscillator, simplifying the control electronics, and flattening of the frequency response of the magnetometer. We demonstrate that self-oscillation does not degrade the performance of the magnetometer in the analog mode and show a practical digital implementation.

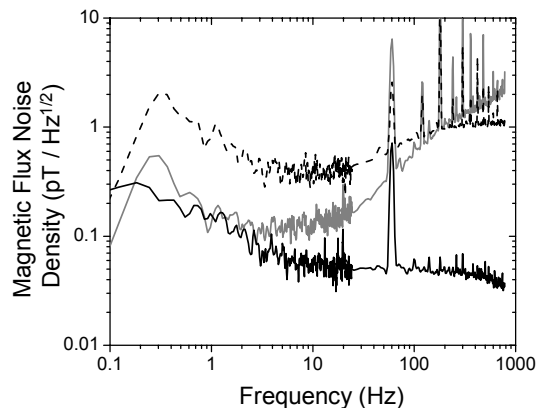


Figure 6. The magnetometer noise spectra for the unlocked mode (black line), the analog self-oscillating mode (gray line), and the digital self-oscillating mode (dashed line) when in a 143 nT field.

shift and gain set appropriately, the system self-oscillates, and the magnetic field is determined by simply counting the frequency of the analog output. We observe self-oscillation in fields ranging from 35 nT to 35,000 nT, and the sensitivity of the magnetometer in the analog self-oscillating mode is shown in Fig. 6 and is  $\sim 0.15 \text{ pT Hz}^{-1/2}$  at 1 Hz bandwidth.

A comparison of the noise spectra of the magnetometer (Fig. 6) shows that at frequencies above 20 Hz the noise in the analog self-oscillating mode increases proportionally to the frequency, while the noise in the unlocked mode is approximately white. This points to another advantage of the self-oscillator—the gain in the self-oscillating loop flattens the frequency response of the system, where as the response in the unlocked mode falls off with the frequency above 20 Hz. Thus, the signal-to-noise ratio at a given frequency in both modes is equivalent.

An obvious disadvantage of the present analog self-oscillating mode is that the low-pass filter needs to be tuned as the magnetic field changes. To avoid this problem, we implemented a digital phase-locked loop (PLL) to lock a voltage controlled oscillator (VCO) to the FM NMOR signal. In this digital self-oscillating mode, we digitally synthesize a sine wave for feedback to the VCSEL with the appropriate phase shift from the locked VCO signal. We find that with the magnetometer in the digital self-oscillating mode the PLL can acquire and track the FM NMOR oscillation frequency over the full locking range of the PLL. The magnetic field is found by counting the frequency of the VCO, and the sensitivity is plotted in Fig. 6 and is  $\sim 0.8 \text{ pT Hz}^{-1/2}$  at 1 Hz bandwidth. The sensitivity of the digital self-oscillating mode is degraded somewhat because the PLL was not properly optimized. The PLL and sine generator are easily implemented with five low-cost, off-the-shelf integrated circuits. With more carefully designed electronics, the sensitivity should be equivalent to the other two methods, and the size and power consumption of the electronics could be greatly reduced for use in a CSAM.

## ACKNOWLEDGEMENTS

We thank H. G. Robinson and M. Prouty for valuable advice. This work is a contribution NIST, an agency of the US government and is not subject to copyright.

## REFERENCES

- [1] P. D. D. Schwindt, *et al.*, “Chip-scale atomic magnetometer,” *Appl. Phys. Lett.*, vol. 85, pp. 6409-6411, 2004.
- [2] B. S. P. Sarma, B. K. Verma, S. V. Satyanarayana, “Magnetic mapping of Majhgawan diamond pipe of central India,” *Geophysics*, vol. 64, pp. 1735-1739, 1999.
- [3] G. Bison, R. Wynands, A. Weis, “A laser-pumped magnetometer for the mapping of human cardiomagnetic fields,” *Appl. Phys. B*, vol. 76, pp. 325-328, 2003.
- [4] A. L. Bloom, “Principles of operation of the rubidium vapor magnetometer,” *Appl. Opt.*, vol. 1, pp. 61-68, 1962; E. B. Alexandrov, M. V. Balabas, A. S. Pasgalev, A. K. Vershovskii, N. N. Yakobson, “Double-resonance atomic magnetometers: From gas discharge to laser pumping,” *Laser Phys.*, vol. 6, pp. 244-251, 1996; I. K. Kominis, T. W. Kornack, J. C. Allred, M. V. Romalis, “A subfemtotesla multichannel atomic magnetometer,” *Nature*, vol. 422, pp. 596, 2003.
- [5] S. Knappe, *et al.*, “A microfabricated atomic clock,” *Appl. Phys. Lett.*, vol. 85, pp. 1460-1462, 2004.
- [6] M. Stahler, S. Knappe, C. Affolderbach, W. Kemp, R. Wynands, “Picotesla magnetometry with coherent dark states,” *Europhys. Lett.*, vol. 54, pp. 323, 2001.
- [7] D. Budker, D. F. Kimball, V. V. Yashchuk, M. Zolotarev, “Nonlinear magneto-optical rotation with frequency-modulated light,” *Phys. Rev. A*, vol. 65, pp. 055403, 2002.
- [8] P. D. D. Schwindt, L. Hollberg, J. Kitching, “Self-oscillating rubidium magnetometer using nonlinear magneto-optical rotation,” unpublished.
- [9] L.-A. Liew, S. Knappe, J. Moreland, H. Robinson, L. Hollberg and J. Kitching, “Microfabricated alkali atom vapor cells,” *Appl. Phys. Lett.*, vol. 84, pp. 2694-2696, 2004.
- [10] R. Lutwak, *et al.*, “The chip-scale atomic clock - low-power physics package,” in 36th Annual Precise Time and Time Interval (PTTI) Meeting. Washington, DC, 2004.
- [11] A. Brannon, J. Breitbarth, and Z. Popovic, “A Low-Power, Low Phase Noise Local Oscillator for Chip-Scale Atomic Clocks,” *IEEE Microwave Theory and Techniques Symposium*, in press, 2005.